OMICS A Journal of Integrative Biology
Volume 23, Number 5, 2019
© Mary Ann Liebert, Inc.
DOI: 10.1089/omi.2019.0011

Research Articles

Skin Microbiome Differences in Atopic Dermatitis and Healthy Controls in Egyptian Children and Adults, and Association with Serum Immunoglobulin E

Mohammed Ramadan,[1] Samar Solyman,[2] Mamdouh Yones,[1] Yasser Abdallah,[3] Hamada Halaby,[1] and Amro Hanora[2]

Downloaded by UNIV OF LIVERPOOL from www.liebertpub.com at 05/18/19. For personal use only.

Abstract

Atopic dermatitis (AD) is a complex, multifactorial, chronic pruritic inflammatory skin disease. We report the first microbiome study and new insights on the relationship between skin microbiota variation and AD susceptibility in a population sample from Egypt. We characterized the skin microbiome in 75 patients with AD and 20 healthy controls using Illumina MiSeq sequencing of 16S rRNA gene. Overall, bacterial diversity of skin microbiome in patients with AD was less than those of the healthy subjects. Genus level analysis revealed significant abundance variations by age, disease severity, locality, or immune response. Among these genera, *Streptococcus*, *Cutibacterium*, and *Corynebacterium* appeared to be specific signatures for AD in children, adolescents, and adults, respectively, while *Staphylococcus* was noted as a potential biomarker candidate for AD. Additionally, functional potential of metagenomes shifted the overall metabolic pathways to participate in the exacerbation of disease. Total immunoglobulin E (IgE) levels were positively correlated with relative enrichment of certain *Staphylococcus aureus* subspecies. Finally, AD-related differences in skin bacterial diversity appeared to be in part linked to the serum IgE level. These new observations attest to the promise of microbiome science and metagenomic analysis in AD specifically, and clinical dermatology broadly.

Keywords: atopic dermatitis, biomarkers, Egypt, microbiome, metagenomics

Introduction

ATOPIC DERMATITIS (AD) is a common, relapsing, chronic skin condition characterized by pruritus, erythema, and eczematous skin lesions. AD affects ~10% to 20% of children and 2% to 4.9% of adults worldwide (Barbarot et al., 2018). The onset of AD typically extends through various phases, including infancy, child, adolescence, and adulthood (Mortz et al., 2015; Rajka, 2012).

Skin is the first outer shield of the human body with various anatomical and physiological structures, harboring billions of resident microorganisms, referred to as the microbiota. Skin microbiota shares complex relationships with the host varying from mutual and may extend to hostile relations in certain conditions. Moreover, microbe–microbe interactions orchestrate the overall microbial community composition of skin microbiome by maintaining immune homeostasis and inhibiting the growth of potential pathogens (Huttenhower et al., 2012). Accordingly, several studies provided evidence that correlated the disturbance in the human microbiota with the etiology of allergic diseases (Iwatsuki et al., 2018; Pascal et al., 2018; Weidinger et al., 2013).

Normally functioning skin mainly depends on collaboration between crucial triad, including epidermal barrier, resident microbial communities, and immune cells in shaping and modulation of the immune system. Consequently, impairments of any of these parameters could be contributed to clinical phenotype of AD as well as worsening of the symptomatology of the disease (Wollenberg et al., 2018).

Pathogenesis of AD is a result of interplay between many factors, which play pivotal roles in the development and modulation of AD, such as genetic predisposition represented in loss-of-function mutation in filaggrin reportedly contributes to exacerbation of the disease by barrier impairment and loss of skin integrity (Scheerer et al., 2018; Thomsen, 2015). Epigenetic and environmental stimuli as well as skin resident

[1]Department of Microbiology and Immunology, Faculty of Pharmacy, Al-Azhar University, Assiut, Egypt.
[2]Department of Microbiology and Immunology, Faculty of Pharmacy, Suez Canal University, Ismaillia, Egypt.
[3]Department of Dermatology, Faculty of Medicine, Al-Azhar University, Assiut, Egypt.

Downloaded by UNIV OF LIVERPOOL from www.liebertpub.com at 05/18/19. For personal use only.

bacteria are also implicated in the pathogenesis of AD (Clausen et al., 2018; Leyden et al., 1974; Rodriguez et al., 2014; Sasaki et al., 2016).

Traditional culture-based techniques for describing the composition of skin bacterial communities are unable to offer optimal description of these communities. On the other hand, the advances in next-generation sequencing have revolutionized the era of microbiome revealing vastly greater bacterial diversity and providing deeper understanding about the relation between community members and the degree of symbiosis provoked on skin with AD (Byrd et al., 2017; Metzker, 2005; Zhang et al., 2011).

Recently, AD has shown to be steadily increasing worldwide (Clausen et al., 2018; Williams, 1992). The adverse impact of AD on quality of life is not restricted to developed countries and is a serious public health concern in low- and middle-income countries as well (Goh et al., 2018; Ng et al., 2018; Williams et al., 1999). In the case of Egypt, dermatological studies in different regions have reported the incidence of AD between different age groups to represent 23% of skin lesion (Abdel-Hafez et al., 2003; Yamamah et al., 2012).

On the other hand, metagenomic studies for AD-associated microbiota in Middle Eastern countries, particularly in Egypt, have been thus far limited in contrast to other world regions (Flohr and Mann, 2014; Iwatsuki et al., 2018). The present study aimed to describe patterns in composition, structure, and functional potential in bacterial communities of patients with AD in comparison to healthy subjects using 16S rRNA microbial analysis at different ages. Additionally, we report on the putative links between skin microbiota and serum immunoglobulin E (IgE).

Materials and Methods

Ethics statement

This study was performed according to the principles of the Declaration of Helsinki and approved by the Scientific Research Ethics Committee at the Faculty of Pharmacy, Suez Canal University, Egypt (reference number of 201609 PHDH). The patient or his/her legal guardian provided full informed consent before collection of skin swabs.

Study design and participants

This study is a case–control study of patients with AD and healthy controls. For skin swabbing, patients with AD who have presented to the outpatient Dermatology Clinic at Al-Azhar University Hospital, Assiut (Egypt) were recruited. Participants were diagnosed as AD on the basis of the Hanifin and Rajka criteria (Hanifin and Rajka, 1980). Clinical severity of AD was assessed using the Scoring AD (SCORAD) index (Schallreuter et al., 1993). Parental questionnaires and physical examination were included in assessment of children group. All subjects were either male or female between 2 and 60 years of age.

Exclusion criteria included systemic or local antibiotic use during 3 weeks before the sampling, topical corticosteroid application within 2 weeks before sampling session, and systemic steroids and immunosuppressant administration within 1 month before sampling. Any subject who failed these criteria was excluded. Healthy control subjects enrolled in this study were nonatopic, with similar age to AD subjects, normal serum IgE level, and assessed for the absence of major skin diseases, including previous AD, psoriasis, and rosacea, as well as other atopic manifestations.

According to the SCORAD, patients were classified to three groups: mild (<15), moderate (between 15 and 40), and severe (>40). To assess the patterns of microbiome during different developmental stages, participants were grouped as children (2–12 years), adolescents (13–18 years), and adult (≥19 years).

Sample collection

Subjects with AD were informed to avoid bathing, using topical medications, and emollients at sampling sites for 24 h before sampling. Skin swabs were collected from antecubital fossa (AF) using aseptic techniques. Briefly, sterile cotton-tipped Catch-All swabs (Epicentre Biotechnologies, Madison, WI, USA) were premoistened with a sterile solution of 0.15 M NaCl and 0.1% Tween 20. Swabs were rubbed firmly for 20 sec over 4 cm^2 areas identified as being the most representative of affected skin. Similarly, samples were also collected from the closest unaffected skin area of 10 AD patients and healthy control subjects.

DNA extraction and high-throughput sequencing

Bacterial genomic DNA was extracted from swabs collected from AD patients, healthy subjects, and laboratory control that was also performed on premoistening solution with and without swab to ascertain any potential contaminants, using DNeasy PowerSoil Kit cat no. 12888-100 (Qiagen, Valencia, CA) as recommended by the manufacturer with modifications as previously described (Ramadan et al., 2016). For microbiota profiling, 16S rRNA gene was amplified by polymerase chain reaction (PCR) using primers targeting V1–V3 regions. Illumina adaptor appended to primers (underlined), forward primer 5′ AATGATACGG CGACCACCGAGATCTACAC ATCGTACGTAT GGTA ATTCAATTA CCGCGGCTGCTGG reverse primer 5′ CAA GCAGAAGAC GGCATACGAGAT AACTCTCGAGTCA GTCAGCCGAGTTTGAT CMTGGCTCAG (Allen et al., 2016).

PCR amplification products' size and quality were verified with a 1% agarose gel and Agencourt XP AMPure Beads (Beckman Coulter, USA). Amplicons from negative control were analyzed in parallel with the processing of the samples to detect the presence of contaminants in swabs, extraction reagents, or during PCR mixture setup. Library preparation and sequencing using Illumina MiSeq Platform (Illumina, USA) were accomplished at IGA Technology Services (Udine, Italy).

Serum total IgE assay

Serum samples were collected from all participants to estimate the total IgE level. Total IgE levels were assayed using the ELISA Kit cat. no. 1801-18 (Diagnostic automation/Cortez diagnostics, Inc., USA) as per the manufacturer's instructions. Optical densities were measured using an enzyme-linked immunosorbent assay (ELISA) reader and levels of total IgE were calculated using standard curves performed for ELISA plate. Total IgE levels are represented as IU/mL. A value of ≥150 IU/mL was considered as raised total serum IgE levels.

Downloaded by UNIV OF LIVERPOOL from www.liebertpub.com at 05/18/19. For personal use only.

Data analyses

Row sequence preprocessing was performed depending on ribosomal sequence variants (RSVs), refers to sequences that differ by >1 nucleotide, using Insights Into Microbial Ecology 2 (QIIME2; release 2018.4) (Caporaso et al., 2010) platform with the DADA2 plugin (Callahan et al., 2016).

In brief, demultiplexed paired reads from study samples and negative controls were input for trimming and filtering of reads with a maximum of two expected errors per read (maxEE = 2) and truncation length for forward and reverse reads, 270 and 210, respectively, to remove low-quality bases at the end of the reads. After word, filtered reads were dereplicated to unique sequences, DADA2 error model parameter 1000000 was used by DADA2 inference algorithm to denoise all sequences. Denoised forward and reverse sequences were merged using a minimum overlap of 20 bp and 0 mismatches.

Once RSVs were inferred, potential chimeric sequences were removed to generate high-resolution RSVs. Representative sequence for each RSV was used for taxonomic classification against the SILVA SSU Ref NR dataset v.132 (Quast et al., 2013) using trained Ribosomal Database Project's (RDP's) naive Bayesian classifier at 99% sequence similarity (Wang et al., 2007). Alternatively taxon-independent clustering was performed by ESPRIT-Tree software (Cai and Sun, 2011) to bin sequences into operational taxonomic units (OTUs) by computing k-mer distance between sequences at similarity levels from 99% (species/strain level) to 80% (phylum level).

Staphylococcus *and* Streptococcus *sequence classification to species level*

For species-level designations, a phylogenetic placement method was used, whereby sequences classified as *Staphylococcus* and *Streptococcus* were placed separately onto maximum likelihood phylogeny by pplacer and guppy (Matsen et al., 2010). Species-level assignments of V1–V3 reads using pplacer analysis was in accordance with whole metagenome shotgun sequencing results revealing accurate and correct species classification, especially *Staphylococcus* species (Meisel et al., 2016). Specifically, a high-quality 16S rRNA reference database packages for these genera were created from full-length 16S rRNA gene sequences extracted from RefSeq genomes (as of August 2018) and RDP type species sequences (Release 11.5).

In brief, extracted sequences were processed using MOTHUR (Schloss et al., 2009), were aligned to SILVA database v.132, screened, and clustered. Reference tree was built from each alignment with GTRGAMMA model in RAxML v.8.0.0 (Berger et al., 2011). Reference package was created by Taxtastic suite of tools (taxit v0.3.1; https://github.com/fhcrc/taxtastic) using the aligned reference sequence and tree. Taxonomic classifications were produced with guppy software (guppy is distributed with pplacer) using a most recent common ancestor approach with likelihood score of at least 0.85 and 0.90 for *Staphylococcus* and *Streptococcus*, respectively (Oh et al., 2013).

To predict the functional profile of skin microbiome based on the 16S rRNA gene sequences, Phylogenetic Investigation of Communities by Reconstruction of Unobserved States (PICRUSt) was used (Langille et al., 2013), all denoised, merged, and chimera-checked reads were exported from qiime2 to fasta file using Qiime2 tools export script and used as input by Qiime, v 1.9.1 for closed-ref OTU picking to assign OTUs against Greengenes database (V 13.8) (McDonald et al., 2012) at a 97% identity using UCLUST (Edgar, 2010). *Predict_metagenomes.py* command in PICRUSt used biom file, generated by closed-reference clustering, to predict metabolic functions through mapping the Kyoto Encyclopedia of Genes and Genome (KEGG) Orthology Database at level 3 (Kanehisa and Goto, 2000; Kanehisa et al., 2014).

Significantly different features such as taxa or KEGG pathways between age groups were identified by the linear discriminant analysis (LDA) effective size (LEfSe) (Segata et al., 2011). Only RSV or KEGG metabolic pathways with logarithmic LDA scores >3.0 and $\alpha = 0.05$ were inputted LEfSe (ver. 1.0).

Statistical analysis

Estimates of ecological indices, which included rarefaction curves, number of observed RSVs (species), and Shannon index, representing common measures of alpha diversity, were analyzed within QIIME2 using a random resampling of 36,944 sequences per sample for even sampling depth. In addition, another dataset was used for downstream analysis using all of the quality-filtered reads per sample. Statistical significance of differences among age groups or healthy and diseased patients was estimated using unpaired Wilcoxon rank-sum test and Kruskal–Wallis rank-sum test. All *p*-values were adjusted for multiple comparisons in R using false discovery rate method (Benjamini and Hochberg, 1995).

Beta diversity analyses were estimated to determine phylogenetic distances between communities, including both unweighted and weighted UniFrac distance matrices (Lozupone et al., 2011). Both UniFrac principal coordinates analysis (PCoA) and the Unweighted Pair Group Method with Arithmetic Mean (UPGMA) were performed for interpretation of the UniFrac distance matrix. Phyloseq and ggpubr, R packages were used for calculation and plotting of α and β diversity (McMurdie and Holmes, 2013), except the robustness of the UPGMA tree was estimated using jackknife based on 1000 replicates by input QIIME and running the *jackknifed_beta_diversity.py* workflow.

Finally, significance testing of sample clustering was assessed by Permutational Multivariate Analysis of Variance (ANOVA) (Adonis R, package Vegan) (Anderson, 2001) using the weighted UniFrac distance matrix in QIIME by *compare_categories.py* script. To define the correlations between microbiota and patient clinical metadata, Spearman correlation coefficient was estimated for genera whose mean relative abundance was ≥0.32% using R package, Hamsic (Harrell and Dupont, 2008). SigFeature package was used for selection of significant features between age group using recursive feature elimination-support vector machine (RFE-SVM) (Das and Roychoudhury, 2017). All plots and figures were generated using ggplot2 and ggtree packages.

Availability of Data

The 16SrRNA raw sequence reads that support the findings of this study have been deposited in Sequence Read Archive under accession number PRJNA481999, and are accessible at www.ncbi.nlm.nih.gov/bioproject/PRJNA481999.

Downloaded by UNIV OF LIVERPOOL from www.liebertpub.com at 05/18/19. For personal use only.

Results

Study cohort and sequencing of 16S rRNA gene

To identify patterns of the skin microbiome in relation to AD, clinical specimens were collected from AF, a common site for AD predilection. A total of 75 patients clinically diagnosed with AD were recruited, including 33 children (Children_AD), 12 adolescents (Adolescent), and 30 adults (Adult_AD). As controls, samples were taken from 20 healthy nonatopic volunteers (Children_H and Adult_H) and nonlesional skin regions of 10 AD patients (Children_NL and Adult_NL) (Supplementary Fig. S1). Demographic data as well as clinical assessments were collected, including age (19.25 ± 15.77) (mean/standard deviation [SD]), and gender (45 males, 50 females). The AD patients in this study had SCORAD (37.95 ± 15.11) representing moderate-to-severe disease with total serum IgE (377.8 ± 297.7). According to geographic locality, there were 43 and 32 participants with AD from urban and rural regions, respectively (Supplementary Table S1).

In total, 108 samples were derived from the AF of 95 participants. Three laboratory controls were processed for V1–V3 region of 16S rRNA gene by Illumina MiSeq, obtaining 8,128,581 sequencing reads (average reads per sample $77{,}415 \pm$ SD 15,369). Quality control checking of reads resulted in 7,637,126 reads that were denoised, dereplicated, merged, and cleared from chimeric sequences (21.97% of filtered reads) obtaining 5,958,743 bacterial 16S rRNA sequencing reads (73.33% of the total reads) that were used in downstream analyses.

Skin bacterial diversity in healthy controls and patients with AD

The overall taxonomic diversity across skin microbiomes was estimated using different alpha diversity metrics, based on species richness estimating the number of observed RSVs. In total 5401 RSVs were detected that ranged from 257 to 1069 (Fig. 1a). The Shannon index (combining richness and evenness of communities) ranged from 0.926 to 5.63 (Fig. 1b). Notably, results of these measures showed significantly more diverse bacterial communities in healthy skin than those related to AD. Although diversity indices of nonlesional regions were relatively but not significantly lower than those from healthy skin (Wilcoxon test, $p = 0.82$), these regions showed mild but significant increased diversity in comparison to lesions of the same patient.

For elucidation of age-specific patterns of AF microbiomes, alpha diversity was compared between different age groups. Whereas healthy children had the highest alpha diversity followed by healthy adults with significant differences from those with AD (Kruskal–Wallis, $p = 7.17 \times 10^{-9}$). However, adolescents presented intermediate diversity between children and adults with AD, it exhibited nonsignificant difference in comparison to children with AD (Wilcoxon test, $p = 0.68$).

Patterns of beta diversity between samples with respect to community membership and structure were analyzed using both weighted and unweighted UniFrac analyses. Divergences among study groups were shown to be statistically significant in a multivariate ANOVA based on dissimilarities (adonis: $r^2 = 0.031$; $p \leq 0.001$). PCoA of weighted UniFrac analyses revealed distinct significant age-dependent clustering of both healthy and patient groups (Fig. 2). Nevertheless, the UPGMA hierarchical clustering of unweighted UniFrac distances was not consistent with PCoA of weighted UniFrac and showed disease-driven clustering, where samples from AD patients were clustered away from those of healthy subjects (Supplementary Fig. S2). These observations highlighted the essential role of bacterial abundance for describing relation between samples.

Comparative taxonomic profiles of healthy and AD skin microbiomes

To compare taxonomic structure and to estimate the age-related diversification of the AF microbiome in healthy and AD, RSVs were assigned to taxonomy at the most resolvable levels (phylum and genus) based on phylotypes in reference 16S rRNA gene databases. In total, 5401 RSVs were detected in AF skin, which were taxonomically classified into 24 phyla, 53 classes, 119 orders, 285 families, and 716 genera. At the phylum level, the dominant phyla were *Firmicutes* (4.31–87.53%), *Proteobacteria* (1.86–53.91%), *Actinobacteria* (2.27–90.31%), and *Bacteroidetes* (4.21–12.79%), which together represented 97.63% of sequences in our dataset (Fig. 3).

A striking tension existed between *Proteobacteria* and *Firmicutes* in healthy group with a mean average of 42.8% and 40.65%, respectively. The geographic locality of healthy subjects, as a comparative parameter, has elucidated the fluctuating predominance of these phyla, where microbiome of rural individuals was markedly different and showed significantly high abundance of *Proteobacteria*, whereas *Firmicutes* were found to be the most abundant in urban subjects. Comparing the abundance of predominant phyla among age groups revealed that *Firmicutes* showed a significantly higher abundance in children with AD than the other age groups. Although *Actinobacteria* existed with steady relatively low abundance (1.6–12.4%) in all children (healthy and AD), it significantly climbed in AD adults and adolescents as well.

At the genus level, 716 genera were detected in AF skin samples. Thirteen genera were predominant in the healthy group, also found in most of the subjects with AD (Supplementary Fig. S3). Skin microbiome was dominated by *Staphylococcus*, *Streptococcus*, *Cutibacterium* (formerly *Propionibacterium*), *Corynebacterium*, *Bacillus*, and *Klebsiella* with the average abundance ≥1%.

Genera affiliated to *Firmicutes*, including *Staphylococcus*, *Streptococcus*, *Veillonella*, *Gemella*, *Clostridium*, and *Bacillus*, were detected in all samples with highly varying relative abundance ranging from 0.82% to 59.56% of all reads. In comparisons between healthy and diseased groups, *Staphylococcus* and *Streptococcus* were more significantly abundant in diseased subjects with average mean 2.3–31.44% and 8.92–58.46%, respectively, whereas in healthy subjects was detected with low relative abundance 1.2–7.6% and 3.5–12.7%, respectively. In addition, representation of *Streptococcus* was significantly decreased in the older groups compared with children (Supplementary Fig. S3).

Although, proteobacterial genera, including *Klebsiella*, *Pseudomonas*, and *Paracocus*, were significantly abundant in healthy controls, they were detected with lower representation in AD patients especially urban ones. Notably, a

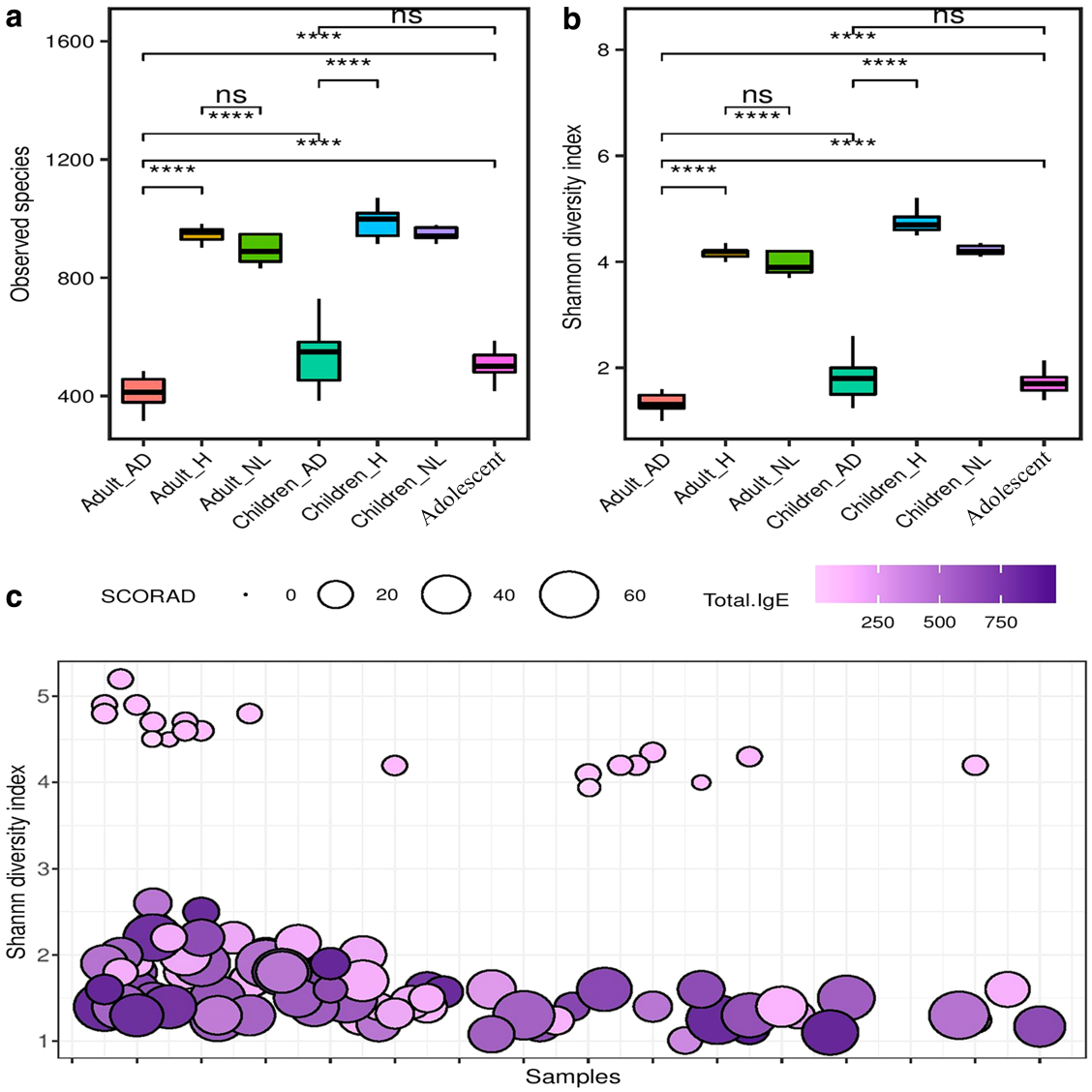


FIG. 1. Alpha diversity indices of cutaneous microbiota. Box plots of Alpha diversity indices were estimated by **(a)** bacterial richness measured as observed species, and **(b)** Shannon diversity index for each age group in healthy controls and subjects with AD. The line in each box plot defines the median, the box delimits the interquartile range (IQR) between the 25th and 75th percentile, and the whisker represents the range. The *x*-axis shows age groups and the *y*-axis shows the observed species (RSVs) in **(a)** and Shannon index in **(b)**. Statistical testing of pairwise comparisons using the nonparametric Wilcoxon rank-sum test. Significant differences within **(a, b)** are displayed with either (ns <1), $*p<0.05$, $**p<0.01$, or $***p<0.001$. Color of boxes correspond to each age group plotted on *x*-axis (Adult_AD, adult with AD; Adult_H, healthy adult; Adult_NL, adult with nonlesional sample; Children_AD, children with AD; Children_H, healthy children; Children_NL, children with AD nonlesional sample) **(c)** *Dot plot* represent association between bacterial diversity measured as Shannon index (*y*-axis) and disease severity (SCORAD) as well as total IgE level in all samples (*x*-axis). SCORAD of each AD patient is indicated by *circle size*. Nonlesional samples were excluded. The indicator value index represents the serum total IgE level of each patient. AD, atopic dermatitis; IgE, immunoglobulin E; ns, non-significant; RSVs, ribosomal sequence variants; SCORAD, scoring AD.

significant increase in the abundance of the genus *Pseudomonas* was observed in lesions of AD rural patients (Supplementary Fig. S3). Moreover, *Pseudomonas* showed inverse significant correlations with other predominant genera, except *Staphylococcus* (Spearman, $r=0.72$, $p<0.01$).

LEfSe analysis was performed for further determination of age-associated differences in bacterial communities and defining taxa that drive taxonomic shifts in healthy and diseased subjects at different developmental stages (Fig. 4 and Supplementary Fig. S4). At the phylum level, *Proteobacteria* and *Actinobacteria* served as strong discriminants for the skin microbiome of AD lesions in children and adolescents, respectively. While at genus level, besides significantly abundant genera in AD, LEfSe also identified discriminative signatures for different health states as well as age-associated microbial profile. In healthy subjects, *Neisseria*, *Paenibacillus*, *Granulicatella*, *Porphyromonas*, and *Enhydrobacter* were identified as potential biomarkers in adult, whereas *Lactococcus* in children.

Downloaded by UNIV OF LIVERPOOL from www.liebertpub.com at 05/18/19. For personal use only.

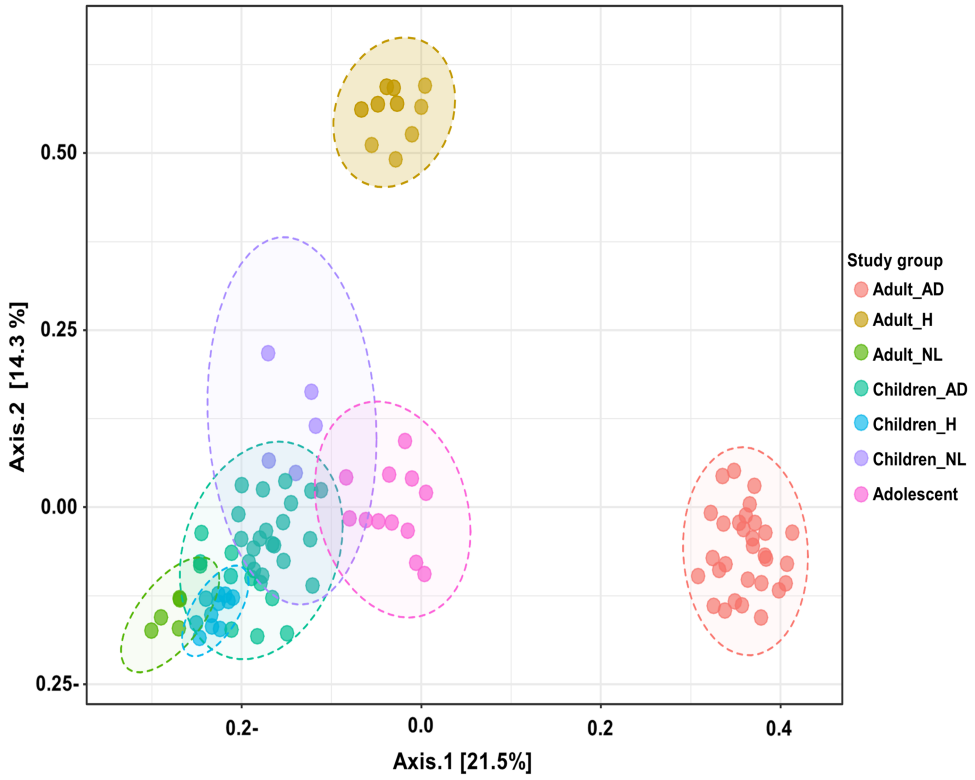


FIG. 2. PCoA for weighted UniFrac distance matrix of cutaneous microbial community structures. Each point on the PCoA plot corresponds to a skin microbiome sample (Adult_AD, adult with AD; Adult_H, healthy adult; Adult_NL, adult with nonlesional sample; Children_AD, children with AD; Children_H, healthy children; Children_NL, children with AD nonlesional sample). The x- and y-axes are indicated by the first and second coordinates, respectively. The percentages of the community variation explained are depicted by the percentages in parentheses on each axis 21.5% and 14.3%, respectively. Ellipses denote significant clustering (p-value <0.001, PERMANOVA) according to age. Color legend indicates age groups in both healthy and AD subjects. PCoA, principal coordinates analysis.

On the other side, skin microbiome of AD subjects showed noticeable shifts emerging in the detection of *Acinetobacter*, *Pseudomonas*, *Staphylococcus*, and *Rothia* that might be candidates as biomarkers for AD in adults. Moreover, *Cutibacterium* and *Prevotella* were identified as microbial signature for AD in adolescents.

Although among the abundant species in healthy rural subjects were *Klebsiella pneumoniae*, *Klebsiella variicola,* and *Bacillus licheniformis*, their proportions were underrepresented in rural patients. On the other hand, *Pseudomonas* species, especially *Pseudomonas aeruginosa* displayed different patterns away from other members of *Proteobacteria*. In healthy subjects, there were faint representation of *P. aeruginosa*, whereas in AD patients its abundance was significantly increased with positive correlations to Staphylococcal species (Spearman, $r \geq 0.68$, $p < 0.01$).

Although *Streptococcus pneumoniae* and *Streptococcus anginosus* were identified as significantly abundant species in healthy and diseased children, their abundance significantly dropped in adolescents and adults. In contrast to Streptococcal species, *Cutibacterium acnes* was detected with low proportions in both healthy and diseased children subjects, while exerted significant elevated abundance in adolescents and adults.

For further studying differences in AD-associated microbiome, similarity distances between lesional and nonlesional region of the same person showed specific microbial signatures. Specifically, *Staphylococcus aureus* showed strongly significant enrichment in AD subjects than healthy controls. In contrast, *Staphylococcus epidermidis* and *C. acnes* were underrepresented in AD lesions compared with nonlesional skin regions.

Although *Staphylococcus* genus was significantly more abundant in AD patients than in healthy controls, classification of *Staphylococcus* to species level highlighted the distinct disease-dependent composition of Staphylococcal communities, where 20 and 35 unique RSVs were assigned to *S. aureus* and *S. epidermidis*, respectively. Interestingly, healthy groups harbored diverse Staphylococcal communities, including *S. epidermidis*, *S. haemoliticus*, *S. cohnii*, *S. aureus*, *S. caprae*, and *S. hominis* (Fig. 5a). On the other hand, AD lesions were primarily colonized with *S. aureus* in addition to *S. caprae*, which was detected with enriched abundance in all samples and inversely correlated with other *Staphylococci*.

For understanding the role of microbe–microbe interaction on microbial community composition as well as pathogenesis of AD, correlations between top 35 genera, present above 0.32% of the total community, were estimated using Spearman correlation coefficient ($r \geq \pm 0.6$, $p \leq 0.01$). In sum, four clusters were identified representing members of the major phyla that significantly correlated in proportion (Fig. 6).

Downloaded by UNIV OF LIVERPOOL from www.liebertpub.com at 05/18/19. For personal use only.

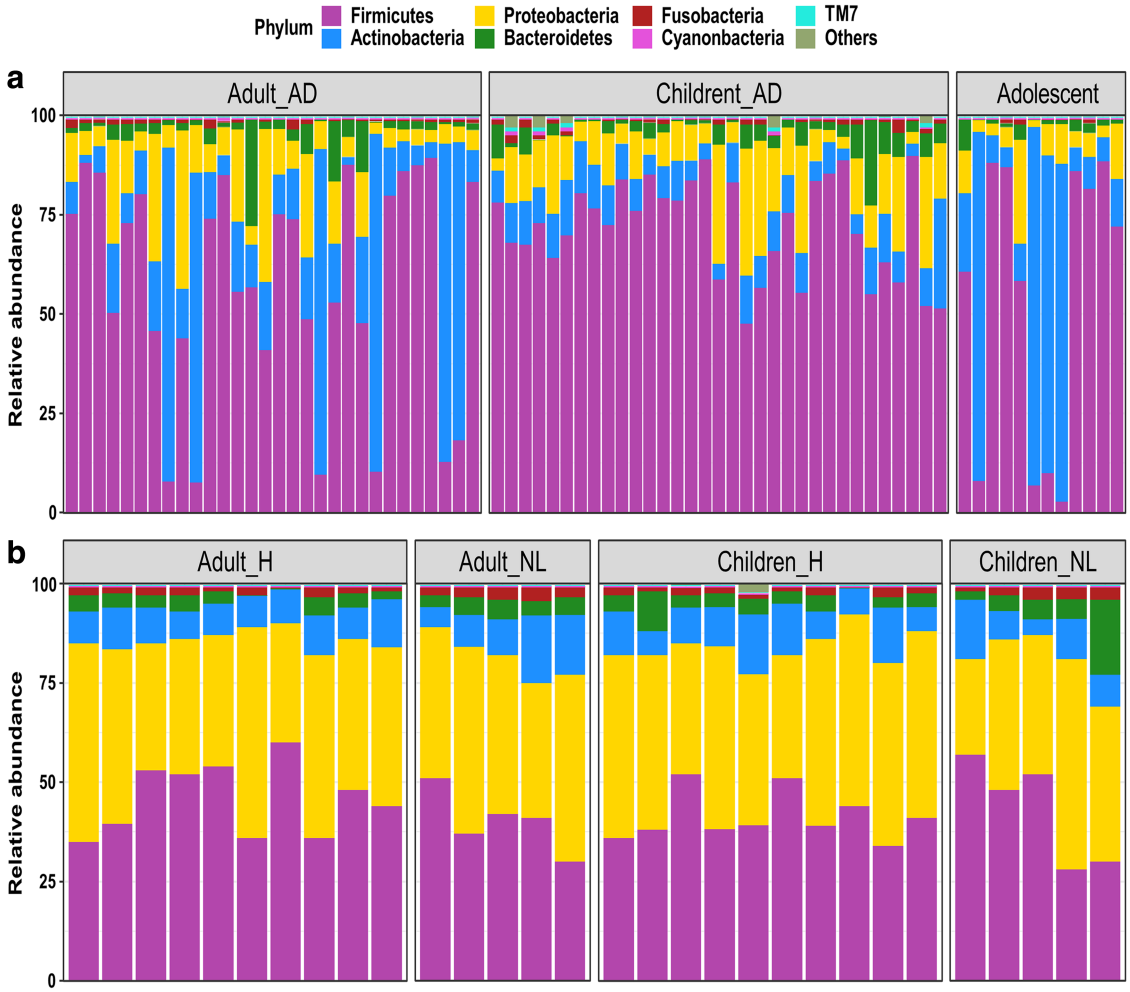


FIG. 3. Phylum taxa level abundance in cutaneous microbiota. Bar charts represent relative proportions of most predominant phyla detected in skin microbiome of patients; with AD at different age groups (**a**) and in healthy nonlesional regions of children and adult subjects (**b**).

Downloaded by UNIV OF LIVERPOOL from www.liebertpub.com at 05/18/19. For personal use only.

Surprisingly, although members of each cluster were positively correlated to each other, *Staphylococcus* was inversely correlated to *Streptococcus*. Correlations between all RSVs in our dataset were also evaluated to define the pairwise relations; altogether 69,423 pairs of significant positive correlations were identified. The strongest positive correlations were noted between RSVs mapped to *S. aureus* and *Anaerococcus*; while 2163 significant negative correlations were detected the strongest were found between RSVs assigned to *Staphylococcus* species (Spearman, $r \geq -0.82$, $p < 0.01$). Strikingly, *S. aureus* RSVs totally inversely correlated to other *Staphylococcus* species, especially *S. epidermidis* and *S. caprae.*

Although *Staphylococcus* genus was strongly correlated to the disease severity (SCORAD), members of genus *Staphylococcus* exhibited distinct correlations, where *S. aureus* positively correlated with disease severity in contrast to other *Staphylococci,* especially *S. epidermidis*.

RFE-SVM analysis was performed on OTUs clustered by ESPRIT-Tree at the 0.03 distance level (OTUs 0.03) to define OTUs that discriminate between AD and healthy microbiota as well as age-specific taxonomic profile. At genus level, most of predictive OTUs between AD and healthy subjects belonged to *Staphylococcus*, *Acinetobacter*, and *Pseudomonas*, whereas OTUs affiliated to *Streptococcus*, *Cutibacterium*, and *Corynebacterium* were distinctive for children, adolescents, and adults, respectively.

Species-level results were in accordance with genus-level analysis, where most discriminative OTUs, clustered by ESPRIT-Tree, were annotated to *S. aureus* that clustered to 115 OTUs at 97% similarity. Phylogenetic tree, based on V1-V3 identity between representative sequences of *S. aureus* clusters, showed distinct clustering of each cluster to 22 clades. Representative sequences of both RSVs and ESPRIT-Tree clusters mapped to *S. aureus* were reclassified producing 20 RSVs that were used for creation of another phylogenetic tree (Fig. 5b).

For further dissecting association between *S. aureus* proportion and total IgE levels, correlation matrix was created between abundance of RSVs mapped to *S. aureus* and total IgE levels (Fig. 5c, d). Total IgE levels remarkably showed positive correlation with relative abundance of six RSVs, whereas the rest of other *S. aureus* RSVs showed positive but not significant correlations to total IgE levels.

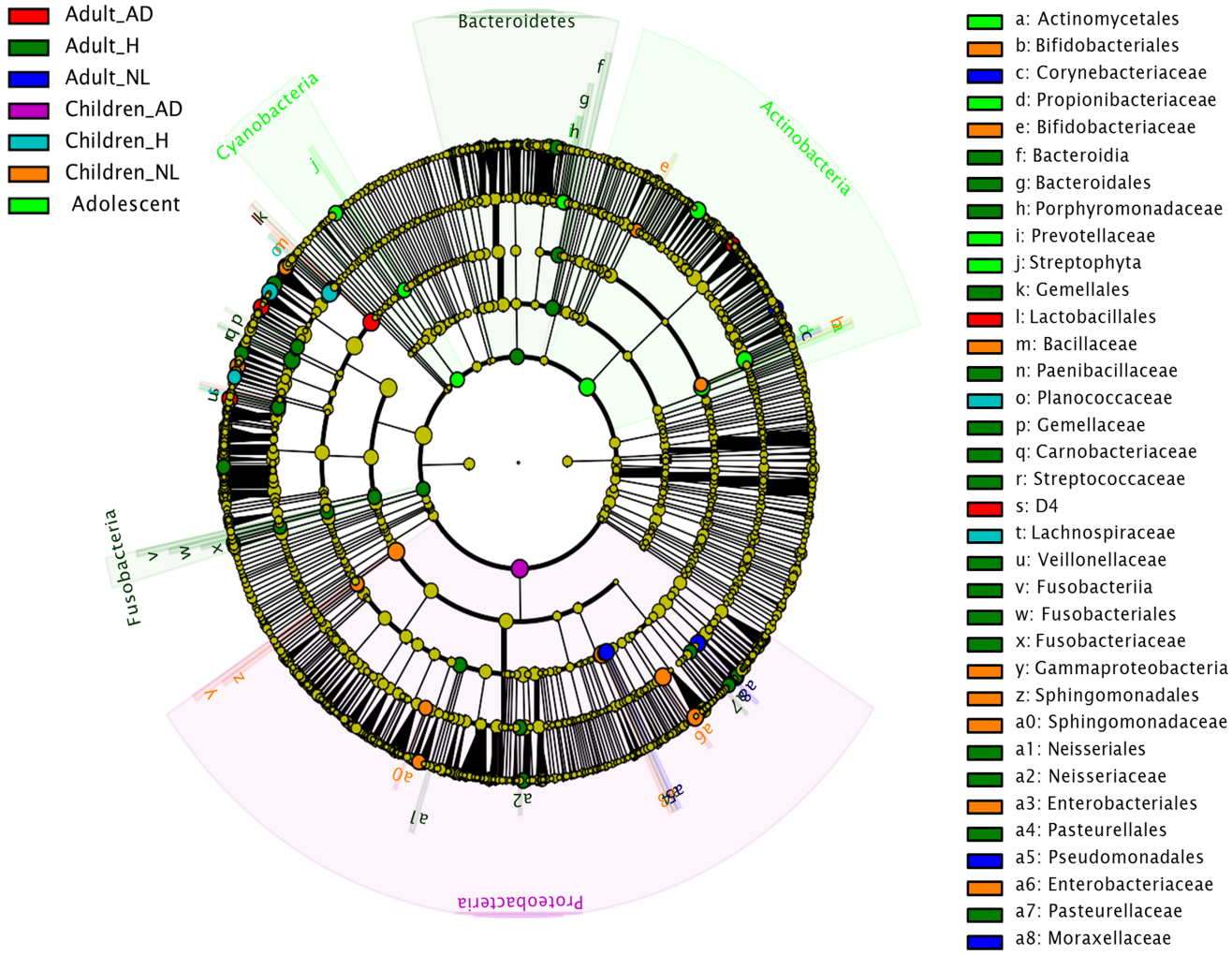


FIG. 4. LEfSe results of cutaneous bacterial communities. Taxonomic cladogram showing significantly abundant taxa that differentiate between AD patients and healthy individuals at different developmental stages. Only taxa with LDA values of 3.0 or higher are shown. Microbial taxa are colored according to age groups in both healthy and AD states (Adult_AD, adult with AD; Adult_H, healthy adult; Adult_NL, adult with nonlesional sample; Children_AD, children with AD; Children_H, healthy children; Children_NL, children with AD nonlesional sample). LDA, linear discriminant analysis; LEfSe, linear discriminant analysis effective size.

Downloaded by UNIV OF LIVERPOOL from www.liebertpub.com at 05/18/19. For personal use only.

Function prediction of bacteria

PICRUSt was used to infer bacterial functions using genomic composition of closely related organisms to the 16S rRNA composition of studied communities. In particular, 21and 58 pathways were significantly enriched in AD patients at level 2 and level 3, respectively (Fig. 7). To a great extent, cutaneous microbiomes in AD patients promoted protein expression of genes associated with amino acid metabolism, lipid metabolism, and pathogenesis-associated proteins as bacterial secretion systems, ribosomes, DNA repair and recombination proteins, and peptidases. Amino acid metabolism included histidine metabolism; alanine, aspartate, and glutamate metabolism; glycine, serine, and threonine metabolism; and arginine and proline metabolism pathways.

Intriguingly, marked lowered levels of potentially beneficial pathways were identified in AD samples, including xenobiotic biodegradation and metabolism, fatty acid biosynthesis, steroid hormone biosynthesis, regulation of actin cytoskeleton, as well as membrane transport and transporters. Otherwise, adolescent-associated bacterial communities showed upregulation of genes related to fatty acid metabolism.

Discussion

AD is a relapsing inflammatory skin disorder affecting both children and adults with increasing prevalence over the world. Thus, more efforts are needed to reveal the etiology and predisposing factors of AD, including cutaneous microbiota. Over the past decade, the advances in high-throughput sequencing platforms have led to comprehensive understanding about the microbial communities that share human body space.

The effective treatment of AD comprises multipronged approaches that aim to alleviate symptoms, decrease inflammation and the recurrence of flare-ups, and combating infection. Furthermore, they involve restoration of normal skin barrier function as well as cutaneous microbial diversity (Wollenberg et al., 2018). The present work was launched to

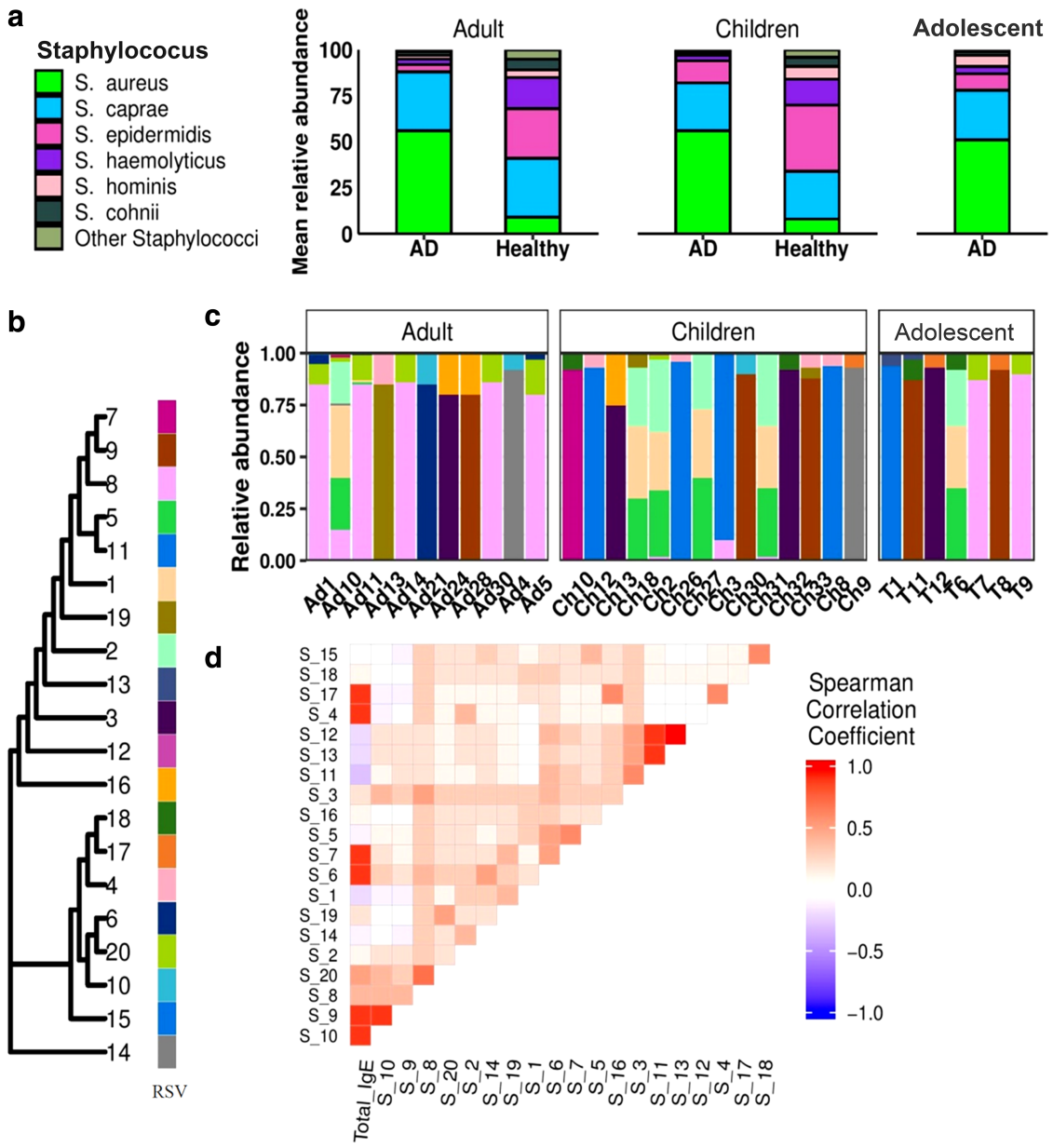


FIG. 5. Average taxonomic composition of Staphylococcal species and correlations of *Staphylococcus aureus* clusters with total IgE. **(a)** Bar chart represents the mean relative abundance of staphylococcal species within staphylococcal communities in antecubital fossa of healthy subjects and AD patients at different age groups. **(b)** Dendrogram based on 16S rRNA similarity of representative reads assigned to *S. aureus* in all samples, each tip is labeled with a number designating corresponding RSV. **(c)** Bar chart represents the relative abundance of RSVs assigned to *S. aureus*, especially in *S. aureus*-enriched AD samples that is plotted on *x*-axis, bar color is corresponding to colored label of each tip in the dendrogram. **(d)** Correlation plot of Spearman coefficient of the relative abundance of RSVs mapped to *S. aureus* and total IgE levels.

profile cutaneous microbiota from patients with AD in different ages in comparison to healthy subjects, with a view to achieve a deeper understanding of disease pathophysiology.

In accordance with previous microbiome studies, a higher bacterial diversity was reported in cutaneous microbiota of healthy subjects than in the AD patients at different disease stages (Byrd et al., 2017; Kong et al., 2012; Shi et al., 2016). The lowered diversity in AD could be attributed to a major factor; pathophysiological alterations in the skin eventually interfere with functions of epidermal barriers. For instance, AD leads to diminished expression of antimicrobial peptides as well as proliferation of keratinocytes, subsequently leading to compositional changes in skin bacterial community (Kong et al., 2012).

Another interesting finding is the intrapersonal variations in patient group, where AD lesions showed significantly lower bacterial diversity than nonlesional regions. These findings were previously linked to AD-associated global alteration in physicochemical properties of skin barrier, such as altered epidermal differentiation, water loss, lipids, and skin pH (van Smeden et al., 2013; Werner and Lindberg, 1985). Furthermore, a strong inverse correlation between disease

Downloaded by UNIV OF LIVERPOOL from www.liebertpub.com at 05/18/19. For personal use only.

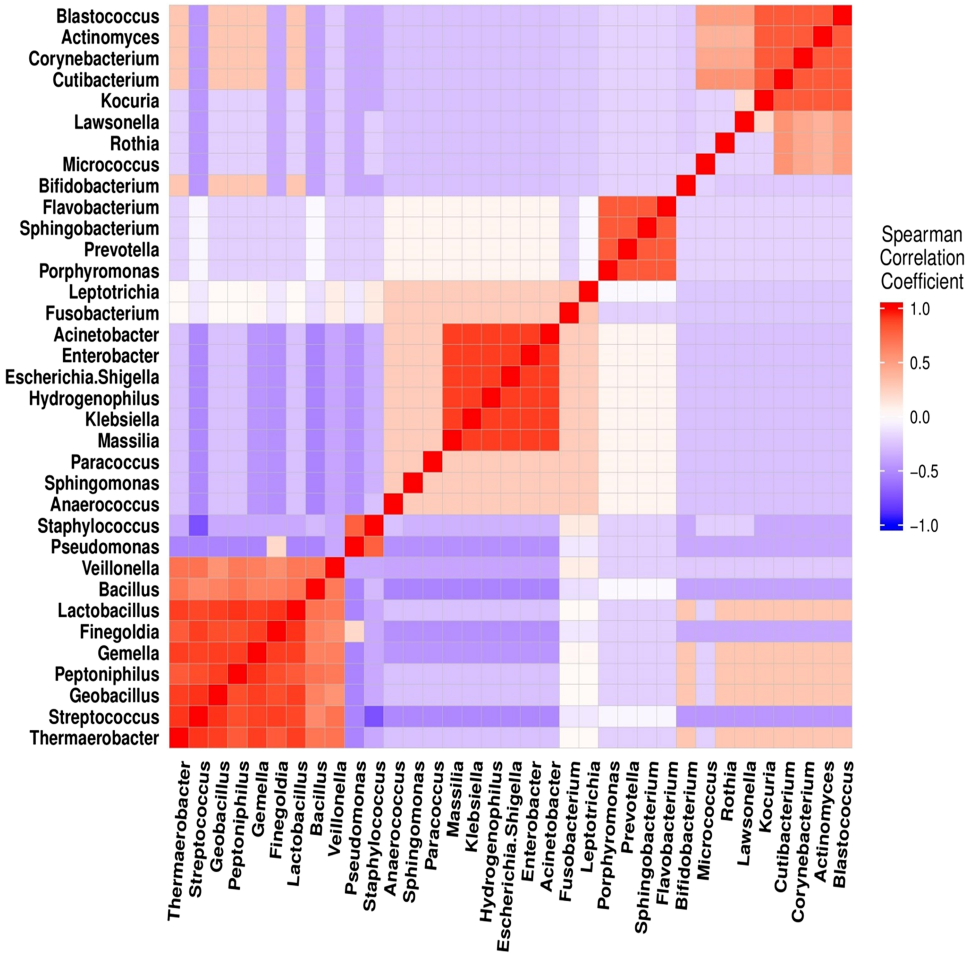


FIG. 6. Correlation plot of pairwise Spearman correlations between the *top* 35 bacterial genera. The heat map scale is color coded by *dark red* for strong positive correlations to *dark blue* for negative correlations.

Downloaded by UNIV OF LIVERPOOL from www.liebertpub.com at 05/18/19. For personal use only.

severity and microbial diversity was found, which matched with previous reports (Byrd et al., 2017; Kong et al., 2012; Shi et al., 2016).

Distinct age-specific shift in skin microbiota is one of the most important findings that was previously reported, probably as a consequence of human developmental stages that extend over maturation-dependent events generating various cutaneous microenvironments with varied physicochemical properties, such as diverse composition and level of sebum production, lipid content, pH, and hair growth (Cotterill et al., 1972; Oh et al., 2012; Shi et al., 2016).

Surprisingly, many studies in the field of AD focused on children, who in spite of AD often continue in adulthood and even in old age (Abrahamsson et al., 2012; Kong et al., 2012; Wang et al., 2008). For further explanation for how age might directly impact the microbiota, adolescent patients were included in this study. The main notable difference between age groups is that the increased representation of genera belonged to *Actinobacteria*, especially *Cutibacterium* and *Corynebacterium*, and was directly linked with progress in age, probably related to physiological and endocrinological changes that accompany maturation. For example, AF has delayed maturation of sebaceous glands and sebum production into adolescence and adulthood.

Among the most abundant phylum in the entire dataset was *Proteobacteria*. It has been previously overrepresented on the skin of rural individuals revealing spatial divergences in the skin microbiome. Furthermore, urban patients with AD showed lower biodiversity than those from rural locations. As a result, surrounding environmental biodiversity has the potential to contribute to variation in skin microbial community (Grice et al., 2008; Hanski et al., 2012; Ramadan et al., 2016; Ying et al., 2015). Moreover, our results revealed significant increase in proportion of *B. licheniformis* in healthy rural controls. This suggests that *B. licheniformis* spores might be an important allergy-protective factor through activation of a TH1 cytokine expression profile (Vogel et al., 2008).

One of the major observations in the current study is the significant overall difference in the representation of the genus *Pseudomonas* between study groups. Additionally, *P. aeruginosa* abundance was correlated to *S. aureus*. In support of our results, *in vitro* wound model reported synergetic bidirectional interplay between them, where *P. aeruginosa* promotes biofilm formation by *S. aureus* as well as inhibiting its phagocytosis (Fugere et al., 2014), while secretion of protein A by *S. aureus* protects *P. aeruginosa* from phagocytosis and interferes with its recognition by neutrophils (Armbruster et al., 2016).

Downloaded by UNIV OF LIVERPOOL from www.liebertpub.com at 05/18/19. For personal use only.

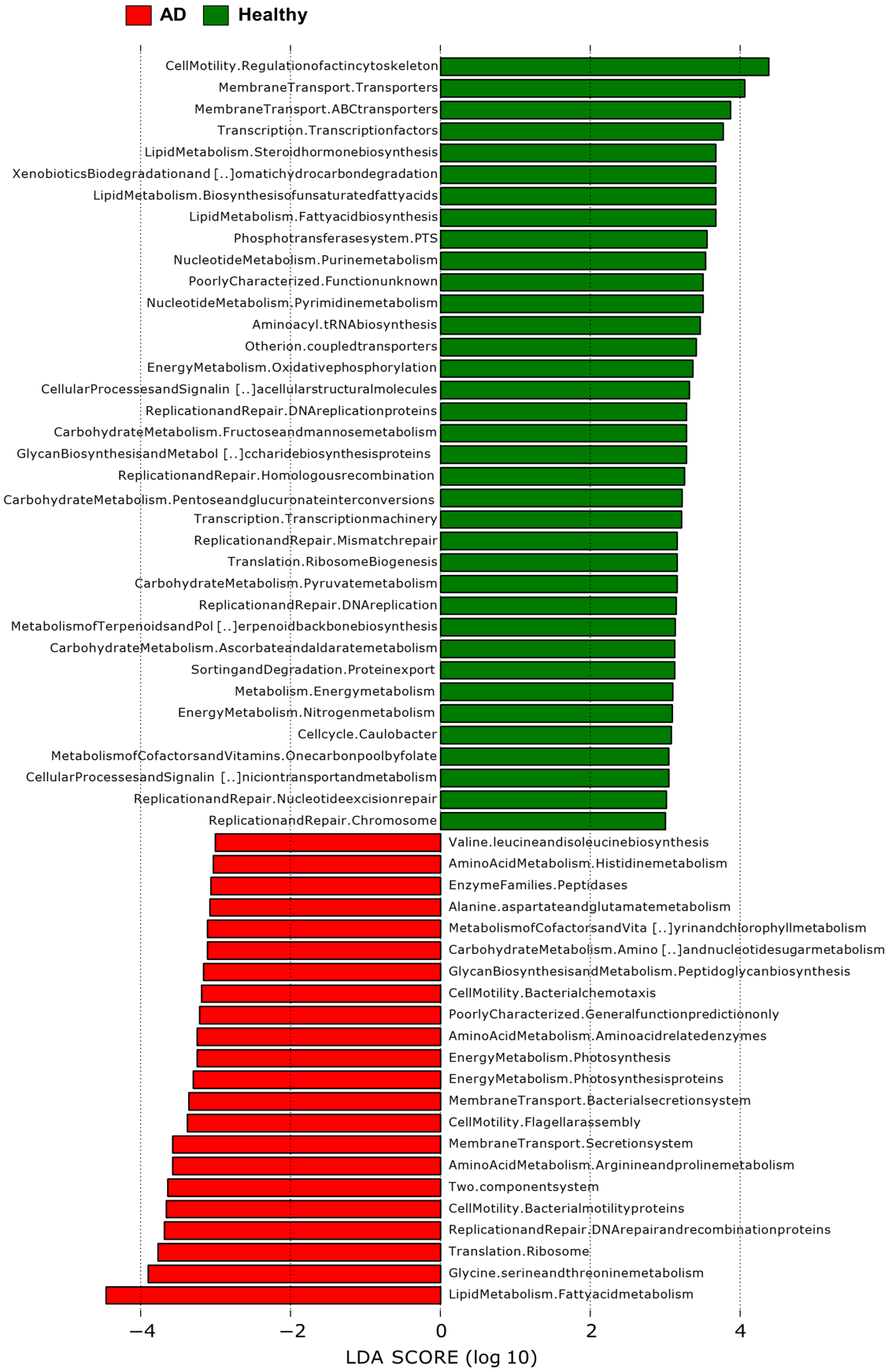


FIG. 7. LEfSe analysis of differentially abundant metabolic pathways between AD and healthy bacterial communities. Histogram of LDA scores computed for metabolic pathways, differently enriched in AD (*red*) and healthy (*green*).

Downloaded by UNIV OF LIVERPOOL from www.liebertpub.com at 05/18/19. For personal use only.

To the best of our knowledge, our findings present the first announcement of *Staphylococcus caprae* in the context of AD. This is rather surprising since *S. caprae* is well described as an animal-associated bacterium, commensal in healthy human skin, and human pathogen especially in nosocomial infections as well (d'Ersu et al., 2016; Moroni et al., 2005; Shuttleworth et al., 1997). It is not clear which mechanism drives the enrichment of *S. caprae* in our AD subjects; however, most likely it is due to the impact of surroundings in shaping microbiota in healthy as well as diseased subjects. Moreover, *S. caprae* has virulent factors which may have a potential role in AD pathogenesis.

For instance, intercellular adhesion genes (ica), are involved in biofilm formation, in addition to atlC gene encoding autolysin that is responsible for binding to fibronectin (Allignet et al., 2001, 2002). In the current study, negative co-occurrence between *S. aureus* and *S. caprae* could be contributed to blocking of agr-mediated quorum sensing of *S. aureus* by *S. caprae* autoinducing peptide (Paharik et al., 2017).

As perturbation in skin pH is one of the most important factors interfering with epidermal functions (Cork et al., 2009), a significant enriched representation of genes related to nitrogen, arginine, and proline metabolism pathways were observed in AD patients. These pathways promote elevation in skin pH through ammonia production, sequentially less acidic skin pH accelerates cascade of changes in epidermal barrier contributing to the phenotype of AD.

A dominant human cutaneous bacterial species is *S. aureus* has been considered as a major player in AD. Increased overall levels of *S. aureus* accompanied with disease severity as well as reduced bacterial diversity due to diminished representation of stabilizer species are in agreement with previous reports (Byrd et al., 2017; Totte et al., 2016; Williams and Gallo, 2015). The second well-defined skin colonizer is *S. epidermidis.* It was detected with retracted abundance in AD patients with nonsignificant association with disease severity in contrast to healthy controls.

Another remarkable finding is the nonsignificant association between total IgE and bacterial diversity (Shannon index) (Fig. 1c). Thus, in the light of this finding, correlation between abundance of total IgE was examined and showed *S. aureus* strain (clade)-dependent elevation in total IgE levels (Fig. 5d). Finally, future studies should be conducted for addressing skin immune response to *S. aureus strains* using animal models and metagenomic approaches.

Conclusions

We have studied skin microbiome associated with AD in comparison to healthy controls. Patients with AD had lower microbial diversity relative to healthy control that may be related to overrepresentation of certain taxa. Taxonomic profiling revealed age-specific microbial signature associated with AD at different ages. Intriguingly, *S. aureus* was detected to be more abundant in both nonlesional and lesional skin of AD subjects. Functional potential investigations of bacterial communities explained shifts in microenvironment and how they directly influence the pathogenesis of AD. Finally, AD-related differences in serum IgE level appeared to be in part linked to certain *S. aureus* subspecies.

Author Disclosure Statement

The authors declare there are no competing financial interests.

Supplementary Material

Supplementary Figure S1
Supplementary Figure S2
Supplementary Figure S3
Supplementary Figure S4
Supplementary Table S1

References

Abdel-Hafez K, Abdel-Aty MA, and Hofny ER. (2003). Prevalence of skin diseases in rural areas of Assiut Governorate, Upper Egypt. Int J Dermatol 42, 887–892.

Abrahamsson TR, Jakobsson HE, Andersson AF, et al. (2012). Low diversity of the gut microbiota in infants with atopic eczema. J Allergy Clin Immunol 129, 434–440, 440.e1–e2.

Allen HK, Bayles DO, Looft T, et al. (2016). Pipeline for amplifying and analyzing amplicons of the V1-V3 region of the 16S rRNA gene. BMC Res Notes 9, 380.

Allignet J, Aubert S, Dyke KG, and El Solh N. (2001). *Staphylococcus caprae* strains carry determinants known to be involved in pathogenicity: A gene encoding an autolysin-binding fibronectin and the ica operon involved in biofilm formation. Infect Immun 69, 712–718.

Allignet J, England P, Old I, and El Solh N. (2002). Several regions of the repeat domain of the *Staphylococcus caprae* autolysin, AtlC, are involved in fibronectin binding. FEMS Microbiol Lett 213, 193–197.

Anderson MJ. (2001). A new method for non-parametric multivariate analysis of variance. Australas Ecol 26, 32–46.

Armbruster CR, Wolter DJ, Mishra M, et al. (2016). *Staphylococcus aureus* protein A mediates interspecies interactions at the cell surface of *Pseudomonas aeruginosa*. MBio 7, e00538–16.

Barbarot S, Auziere S, Gadkari A, et al. (2018). Epidemiology of atopic dermatitis in adults: Results from an international survey. Allergy 73, 1284–1293.

Benjamini Y, and Hochberg Y. (1995). Controlling the false discovery rate: A practical and powerful approach to multiple testing. J R Stat Soc Series B Stat Methodol 57, 289–300.

Berger SA, Krompass D, and Stamatakis A. (2011). Performance, accuracy, and Web server for evolutionary placement of short sequence reads under maximum likelihood. Syst Biol 60, 291–302.

Byrd AL, Deming C, Cassidy SKB, et al. (2017). Staphylococcus aureus and *Staphylococcus epidermidis* strain diversity underlying pediatric atopic dermatitis. Sci Transl Med 9, eaal4651.

Cai Y, and Sun Y. (2011). ESPRIT-Tree: Hierarchical clustering analysis of millions of 16S rRNA pyrosequences in quasilinear computational time. Nucleic Acids Res 39, e95.

Callahan BJ, Mcmurdie PJ, Rosen MJ, et al. (2016). DADA2: High-resolution sample inference from Illumina amplicon data. Nat Methods 13, 581–583.

Caporaso JG, Kuczynski J, Stombaugh J, et al. (2010). QIIME allows analysis of high-throughput community sequencing data. Nat Methods 7, 335–336.

Clausen ML, Agner T, Lilje B, et al. (2018). Association of disease severity with skin microbiome and filaggrin gene mutations in adult atopic dermatitis. JAMA Dermatol 154, 293–300.

Downloaded by UNIV OF LIVERPOOL from www.liebertpub.com at 05/18/19. For personal use only.

Cork MJ, Danby SG, Vasilopoulos Y, et al. (2009). Epidermal barrier dysfunction in atopic dermatitis. J Invest Dermatol 129, 1892–1908.

Cotterill JA, Cunliffe WJ, Williamson B, and Bulusu L. (1972). Age and sex variation in skin surface lipid composition and sebum excretion rate. Br J Dermatol 87, 333–340.

Das P, and Roychoudhury S. (2017). Published. Tripathy, S. sigFeature: An R-package for significant feature selection using SVM-RFE & t-statistic. NGBT conference, Oct. 02-04.

D'ersu J, Aubin GG, Mercier P, et al. (2016). Characterization of *Staphylococcus caprae* clinical isolates involved in human bone and joint infections, compared with goat mastitis isolates. J Clin Microbiol 54, 106–113.

Edgar RC. (2010). Search and clustering orders of magnitude faster than BLAST. Bioinformatics 26, 2460–2461.

Flohr C, and Mann J. (2014). New insights into the epidemiology of childhood atopic dermatitis. Allergy 69, 3–16.

Fugere A, Lalonde Seguin D, Mitchell G, et al. (2014). Interspecific small molecule interactions between clinical isolates of *Pseudomonas aeruginosa* and *Staphylococcus aureus* from adult cystic fibrosis patients. PLoS One 9, e86705.

Goh YY, Keshavarzi F, and Chew YL. (2018). Prevalence of atopic dermatitis and pattern of drug therapy in Malaysian children. Dermatitis 29, 151–161.

Grice EA, Kong HH, Renaud G, et al. (2008). A diversity profile of the human skin microbiota. Genome Res 18, 1043–1050.

Hanifin JM, and Rajka G. (1980). Diagnostic features of atopic dermatitis. Acta Derm Venereol 92, 44–47.

Hanski I, Von Hertzen L, Fyhrquist N, et al. (2012). Environmental biodiversity, human microbiota, and allergy are interrelated. Proc Natl Acad Sci U S A 109, 8334–8339.

Harrell FE, and Dupont CJRPV. (2008). Hmisc: Harrell miscellaneous. R package version 3.

Huttenhower C, Gevers D, Knight R, et al. (2012). Structure, function and diversity of the healthy human microbiome. Nature 486, 207.

Iwatsuki K, Yamasaki O, and Morizane S. (2018). Microbiome, dysbiosis, and atopic dermatitis. *In: Evolution of Atopic Dermatitis in the 21st Century.* Katayama I, Murota H, and Satoh T, eds. Singapore: Springer Singapore.

Kanehisa M, and Goto S. (2000). KEGG: Kyoto encyclopedia of genes and genomes. Nucleic Acids Res 28, 27–30.

Kanehisa M, Goto S, Sato Y, et al. (2014). Data, information, knowledge and principle: Back to metabolism in KEGG. Nucleic Acids Res 42, D199–D205.

Kong HH, Oh J, Deming C, et al. (2012). Temporal shifts in the skin microbiome associated with disease flares and treatment in children with atopic dermatitis. Genome Res 22, 850–859.

Langille MG, Zaneveld J, Caporaso JG, et al. (2013). Predictive functional profiling of microbial communities using 16S rRNA marker gene sequences. Nat Biotechnol 31, 814–821.

Leyden JJ, Marples RR, and Kligman AM. (1974). *Staphylococcus aureus* in the lesions of atopic dermatitis. Br J Dermatol 90, 525–530.

Lozupone C, Lladser ME, Knights D, Stombaugh J, and Knight R. (2011). UniFrac: An effective distance metric for microbial community comparison. ISME J 5, 169–172.

Matsen FA, Kodner RB, and Armbrust EV. (2010). pplacer: Linear time maximum-likelihood and Bayesian phylogenetic placement of sequences onto a fixed reference tree. BMC Bioinformatics 11, 538.

Mcdonald D, Price MN, Goodrich J, et al. (2012). An improved Greengenes taxonomy with explicit ranks for ecological and evolutionary analyses of bacteria and archaea. ISME J 6, 610–618.

Mcmurdie PJ, and Holmes S. (2013). phyloseq: An R package for reproducible interactive analysis and graphics of microbiome census data. PLoS One 8, e61217.

Meisel JS, Hannigan GD, Tyldsley AS, et al. (2016). Skin microbiome surveys are strongly influenced by experimental design. J Invest Dermatol 136, 947–956.

Metzker ML. (2005). Emerging technologies in DNA sequencing. Genome Res 15, 1767–1776.

Moroni P, Pisoni G, Antonini M, et al. (2005). Subclinical mastitis and antimicrobial susceptibility of *Staphylococcus caprae* and *Staphylococcus epidermidis* isolated from two Italian goat herds. J Dairy Sci 88, 1694–1704.

Mortz CG, Andersen KE, Dellgren C, Barington T, and Bindslev-Jensen C. (2015). Atopic dermatitis from adolescence to adulthood in the TOACS cohort: Prevalence, persistence and comorbidities. Allergy 70, 836–845.

Ng MS, Tan S, Chan NH, Foong AY, and Koh MJ. (2018). Effect of atopic dermatitis on quality of life and its psychosocial impact in Asian adolescents. Australas J Dermatol 59, e114–e117.

Oh J, Conlan S, Polley EC, Segre JA, and Kong HH. (2012). Shifts in human skin and nares microbiota of healthy children and adults. Genome Med 4, 77.

Oh J, Freeman AF, Park M, et al. (2013). The altered landscape of the human skin microbiome in patients with primary immunodeficiencies. Genome Res 23, 2103–2114.

Paharik AE, Parlet CP, Chung N, et al. (2017). Coagulase-negative Staphylococcal strain prevents *Staphylococcus aureus* colonization and skin infection by blocking quorum sensing. Cell Host Microbe 22, 746–756.e5.

Pascal M, Perez-Gordo M, Caballero T, et al. (2018). Microbiome and allergic diseases. Front Immunol 9, 1584.

Quast C, Pruesse E, Yilmaz P, et al. (2013). The SILVA ribosomal RNA gene database project: Improved data processing and web-based tools. Nucleic Acids Res 41, D590–D596.

Rajka G. (2012). *Essential Aspects of Atopic Dermatitis*. Springer Science & Business Media, Berlin, Germany.

Ramadan M, Solyman S, Taha M, and Hanora A (2016). Preliminary characterization of human skin microbiome in healthy Egyptian individuals. Cell Mol Biol (Noisy-le-grand) 62, 21–27.

Rodriguez E, Baurecht H, Wahn AF, et al. (2014). An integrated epigenetic and transcriptomic analysis reveals distinct tissue-specific patterns of DNA methylation associated with atopic dermatitis. J Invest Dermatol 134, 1873–1883.

Sasaki M, Yoshida K, Adachi Y, et al. (2016). Environmental factors associated with childhood eczema: Findings from a national web-based survey. Allergol Int 65, 420–424.

Schallreuter K, Levenig C, Berger J, et al. (1993). Severity scoring of atopic dermatitis: The SCORAD index. Dermatology 186, 23–31.

Scheerer C, Eyerich KJDH, and Zeitschrift Fur Dermatologie V, Und Verwandte Gebiete (2018). Pathogenesis of atopic dermatitis. Der Hautarzt; Zeitschrift fur Dermatologie, Venerologie, und verwandte Gebiete. Hautarzt 69, 191–196.

Schloss PD, Westcott SL, Ryabin T, et al. (2009). Introducing mothur: Open-source, platform-independent, community-supported software for describing and comparing microbial communities. Appl Environ Microbiol 75, 7537–7541.

Segata N, Izard J, Waldron L, et al. (2011). Metagenomic biomarker discovery and explanation. Genome Biol 12, R60.
Shi B, Bangayan NJ, Curd E, et al. (2016). The skin microbiome is different in pediatric versus adult atopic dermatitis. J Allergy Clin Immunol 138, 1233–1236.
Shuttleworth R, Behme RJ, Mcnabb A, and Colby WD. (1997). Human isolates of *Staphylococcus caprae*: Association with bone and joint infections. J Clin Microbiol 35, 2537–2541.
Thomsen SF. (2015). The contribution of twin studies to the understanding of the aetiology of asthma and atopic diseases. Eur Clin Respir J 2, 27803.
Totte JE, Van Der Feltz WT, Hennekam M, et al. (2016). Prevalence and odds of *Staphylococcus aureus* carriage in atopic dermatitis: A systematic review and meta-analysis. Br J Dermatol 175, 687–695.
Van Smeden J, Janssens M, Lavrijsen AP, et al. (2013). Skin barrier dysfunction in non-lesional atopic eczema: The role of stratum corneum lipids. Eur J Dermatol. (Ahead of print).
Vogel K, Blumer N, Korthals M, et al. (2008). Animal shed *Bacillus licheniformis* spores possess allergy-protective as well as inflammatory properties. J Allergy Clin Immunol 122, 307–312, 312.e1–e8.
Wang M, Karlsson C, Olsson C, et al. (2008). Reduced diversity in the early fecal microbiota of infants with atopic eczema. J Allergy Clin Immunol 121, 129–134.
Wang Q, Garrity GM, Tiedje JM, and Cole JR. (2007). Naive Bayesian classifier for rapid assignment of rRNA sequences into the new bacterial taxonomy. Appl Environ Microbiol 73, 5261–5267.
Weidinger S, Willis-Owen SA, Kamatani Y, et al. (2013). A genome-wide association study of atopic dermatitis identifies loci with overlapping effects on asthma and psoriasis. Hum Mol Genet 22, 4841–4856.
Werner Y, and Lindberg M. (1985). Transepidermal water loss in dry and clinically normal skin in patients with atopic dermatitis. Acta Derm Venereol 65, 102–105.
Williams H, Robertson C, Stewart A, et al. (1999). Worldwide variations in the prevalence of symptoms of atopic eczema in the International Study of Asthma and Allergies in Childhood. J Allergy Clin Immunol 103, 125–138.
Williams HC. (1992). Is the prevalence of atopic dermatitis increasing? Clin Exp Dermatol 17, 385–391.
Williams MR, and Gallo RL. (2015). The role of the skin microbiome in atopic dermatitis. Curr Allergy Asthma Rep 15, 65.
Wollenberg A, Barbarot S, Bieber T, et al. (2018). Consensus-based European guidelines for treatment of atopic eczema (atopic dermatitis) in adults and children: Part II. J Eur Acad Dermatol Venereol 32, 850–878.
Yamamah GA, Emam HM, Abdelhamid MF, et al. (2012). Epidemiologic study of dermatologic disorders among children in South Sinai, Egypt. Int J Dermatol 51, 1180–1185.
Ying S, Zeng DN, Chi L, et al. (2015). The influence of age and gender on skin-associated microbial communities in urban and rural human populations. PLoS One 10, e0141842.
Zhang J, Chiodini R, Badr A, and Zhang G. (2011). The impact of next-generation sequencing on genomics. J Genet Genomics 38, 95–109.

Address correspondence to:
Amro Hanora, PhD
Department of Microbiology and Immunology
Faculty of Pharmacy
Suez Canal University
Ismaillia 41522
Egypt

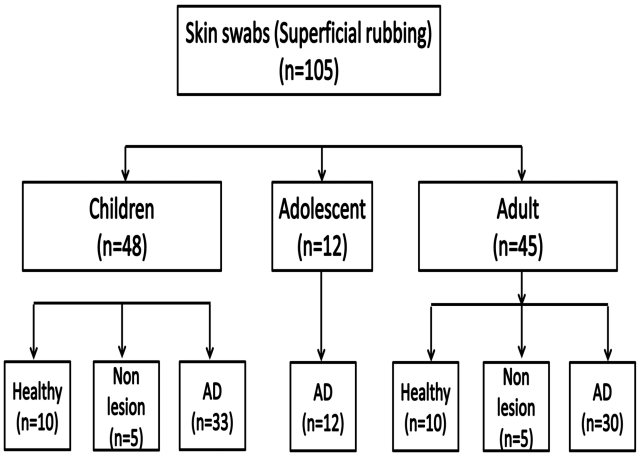
E-mail: ahanora@yahoo.com

Abbreviations Used

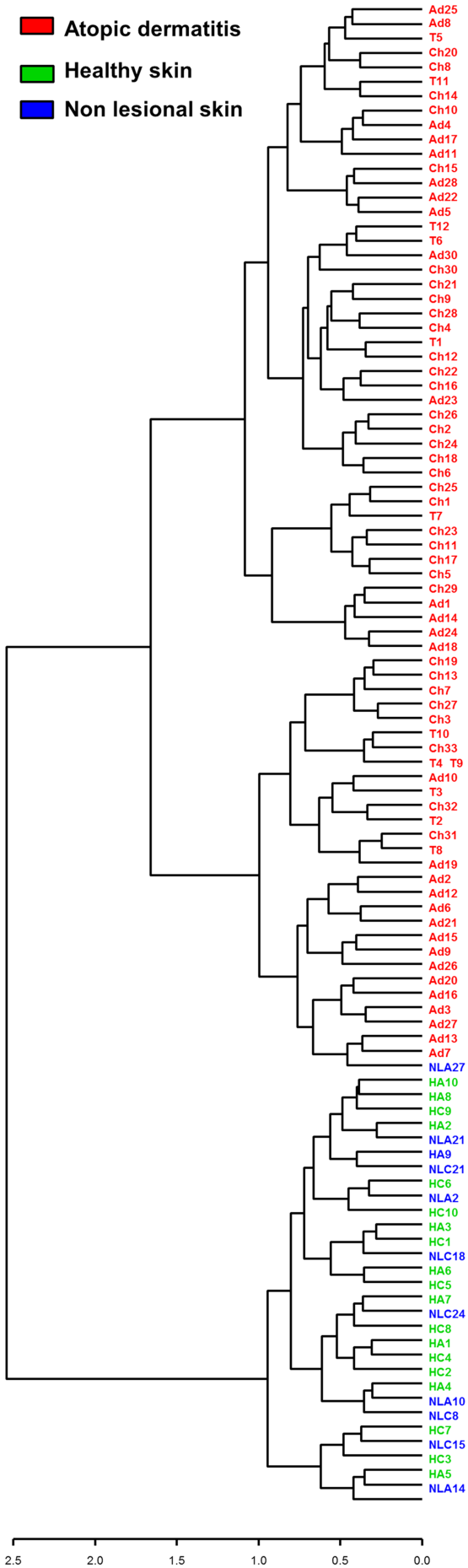
AD = atopic dermatitis
Adult_AD = adult with AD
Adult_H = healthy adult
Adult_NL = adult with AD nonlesional sample
ANOVA = analysis of variance
Children_AD = children with AD
Children_H = healthy children
Children_NL = children with AD nonlesional sample
ELISA = enzyme-linked immunosorbent assay
IgE = immunoglobulin E
KEGG = kyoto encyclopedia of genes and genome
LDA = linear discriminant analysis
LEfSe = linear discriminant analysis effective size
NA = non-applicable
ns = non-significant
OTU = operational taxonomic unit
PCoA = principle coordinate analysis
PCR = polymerase chain reaction
PICRUSt = Phylogenetic Investigation of Communities by Reconstruction of Unobserved States
QIIME2 = quantitative insights into microbial ecology 2
RDP = Ribosomal Database Project
RFE-SVM = recursive feature elimination-support vector macine
RSV = ribosomal sequence variant
SCORAD = scoring AD
SD = standard deviation
UPGMA = unweighted pair group method with arithmetic mean

Downloaded by UNIV OF LIVERPOOL from www.liebertpub.com at 05/18/19. For personal use only.

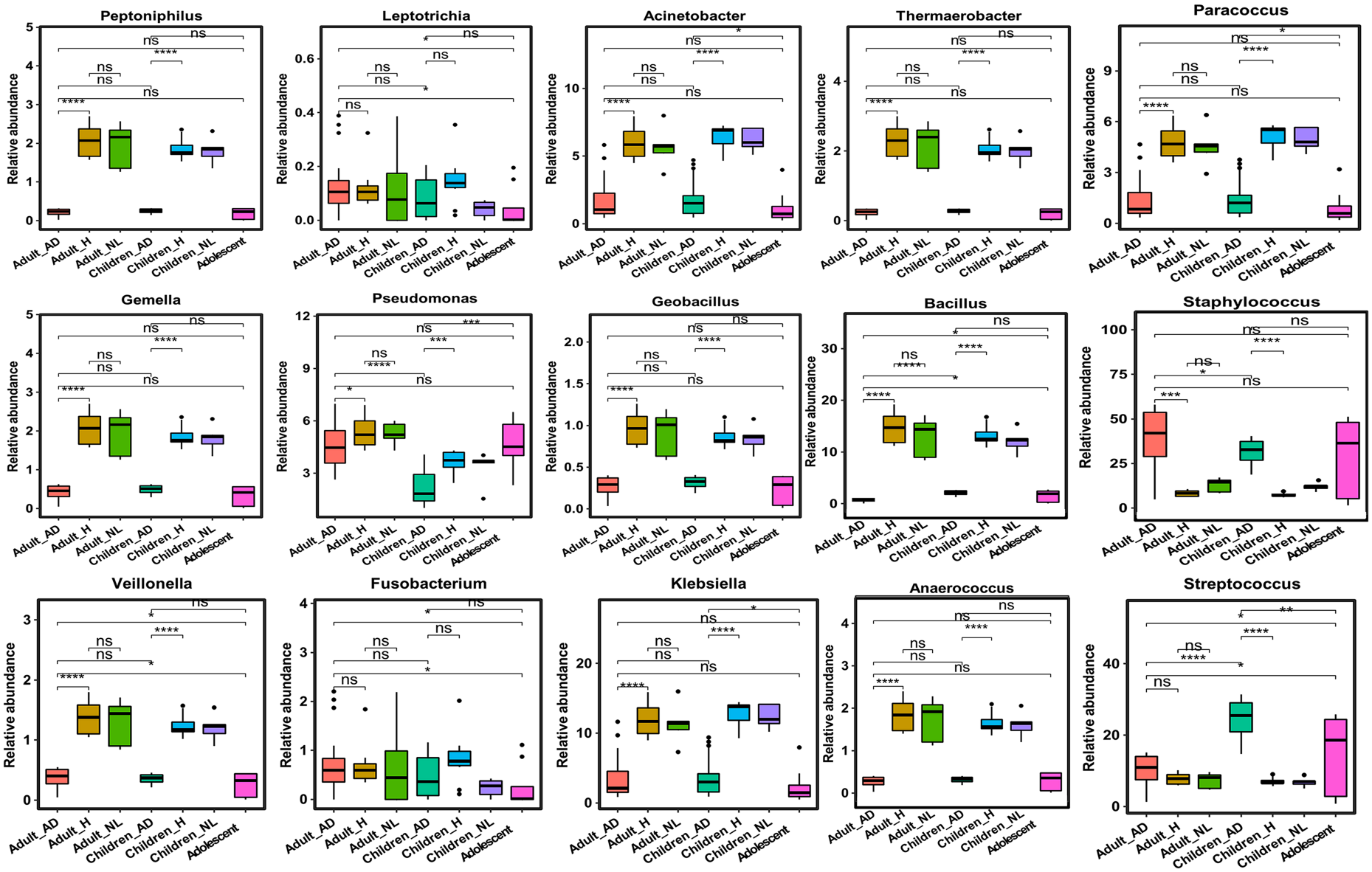
Supplementary Data



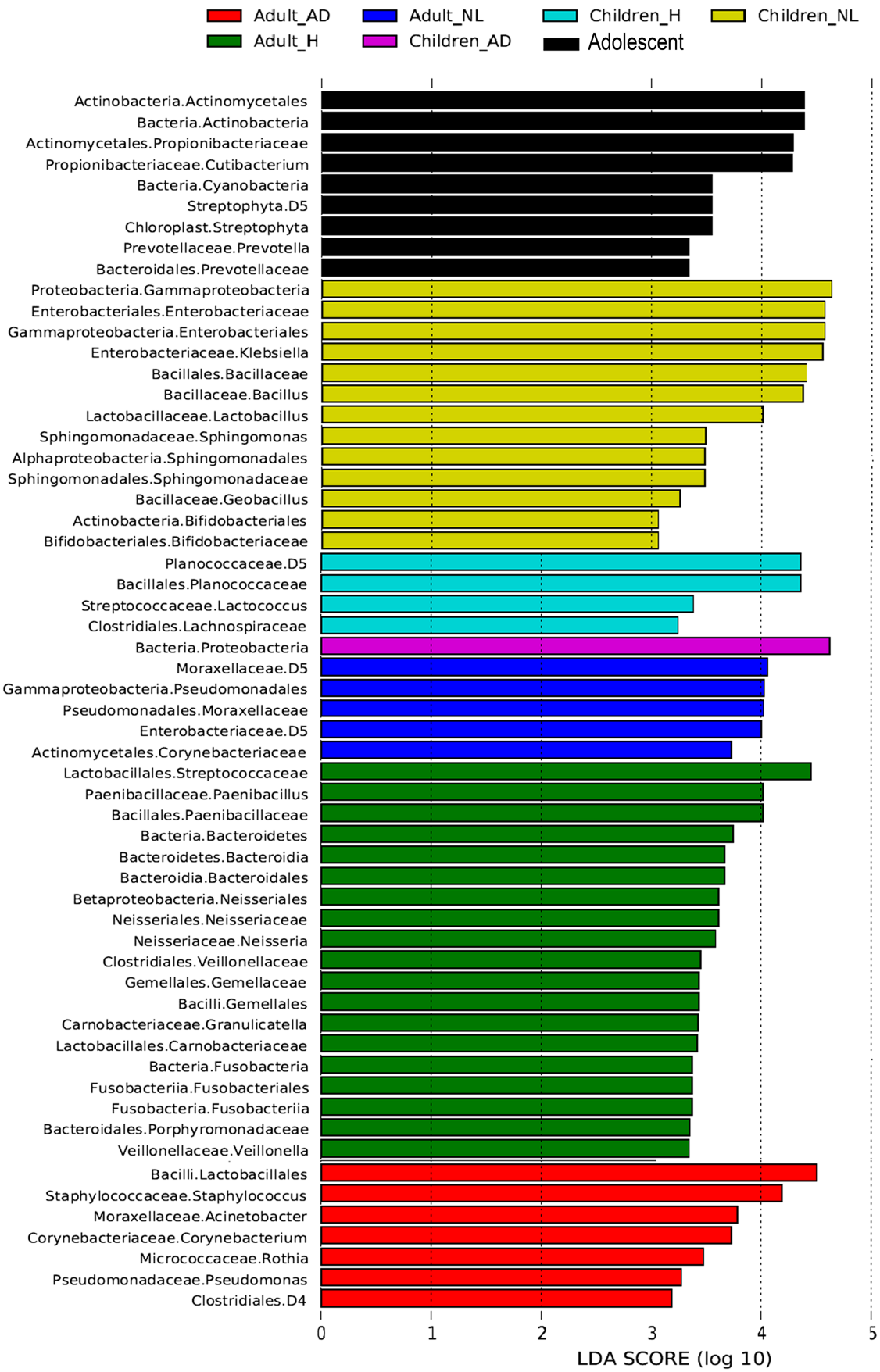
SUPPLEMENTARY FIG. S1. Study design chart explaining the number of collected samples from each study group.



SUPPLEMENTARY FIG. S2. UniFrac-based UPGMA cluster dendrogram of cutaneous microbiota. Skin samples showed disease-based clustering, where samples from subjects with AD (Ad, adult samples; Ch, children samples; T, adolescent samples), clustered together away from both healthy (HA, healthy adult; HC, healthy child) and nonlesional skin regions (NLA, nonlesional adult sample; NLC, nonlesional sample from children). AD, atopic dermatitis.



SUPPLEMENTARY FIG. S3. Relative abundance of the most predominant genera. Box plots show bacterial genera that showed significant differences in abundance between healthy and AD subjects at different age groups. Asterisks indicate significant differences (ns, $p > 1$; *$p < 0.05$; **$p < 0.01$; ***$p < 0.001$; ****$p < 0.0001$).



SUPPLEMENTARY FIG. S4. Histogram of discriminative taxa between microbiome in healthy and diseased subjects based on LEfSe analysis. LDA scores calculated for bacterial taxa that significantly differed in healthy and AD subjects at different age groups (Adult_AD, adult with AD; Adult_H, healthy adult; Adult_NL, adult with nonlesional sample; Children_AD, children with AD; Children_H, healthy children; Children_NL, children with AD nonlesional sample). LDA, linear discriminant analysis; LEfSe, linear discriminant analysis effective size.

Supplementary Table S1. Demographic Data and Clinical Assessment of Healthy Controls and Patients with Atopic Dermatitis

Parameter	*AD patients*	*Control subjects*
Subjects analyzed	75	20
Mean age ± SD (years)	19.25 ± 15.77	20.2 ± 16.4
Male	35	10
Female	40	10
Male/female	0.875	1
Geographic location		
Urban	43	10
Rural	32	10
Objective SCORAD (median) (mild/moderate/severe)	0/36/39	NA
Family history		
Yes	19	NA
No	56	20
IgE in IU/mL (median)	550	41

AD, atopic dermatitis; IgE, immunoglobulin E; NA, non-applicable; SCORAD, scoring AD; SD, standard deviation.